INTERNATIONAL RESEARCH JOURNAL OF ENGINEERING AND TECHNOLOGY (IRJET) E-ISSN: 2395-0056
VOLUME: 07, SPECIAL ISSUE | JUNE 2020 WWW.IRJET.NET P-ISSN: 2395-0072
International Conference on Recent Trends in Science & Technology-2020 (ICRTST - 2020)
Organised by: ATME College of Engineering, Mysuru, INDIA

Enhanced Photocatalytic Degradation of Rhodamine B using Porous Tricobalt Tetraoxide Nanoparticles

Sujay Shekar G. C[1]., Khaled Alkanad[2] and Lokanath N. K[3]
Department of Studies in Physics, Manasagangotri, University of Mysore, Mysuru, India – 570006

Abdo Hezam[4]
Center of Materials Science and Technology, Vijana Bhavana, University of Mysore, Mysuru, India – 570006

Abstract— Porous Co_3O_4 nanoparticles were synthesized using solution combustion method. Cobalt nitrate and glycine were used as oxidizing agents and fuel respectively. The processed sample was calcinated at 600° C for 2 h to eliminate the impurities. We studied Structural, optical and morphological properties using X-ray diffraction (XRD), Dynamic light scattering (DLS), Raman spectroscopy, Scanning electron microscope (SEM), Energy dispersive X-ray analysis (EDAX) and Ultra violet-visible absorption spectroscopy. The XRD data confirmed that Co_3O_4 nanoparticles are crystallized as face-centered cubic (Fd3m) structure. The microstructural and particulate studies showed the presence of porous nanoparticles structure in the samples. The Co and O atomic concentrations were estimated to be 39% and 61% respectively in the sample. The porous Co_3O_4 nanoparticles show two band gap energy 1.58 and 2.05 eV. Photocatalytic degradation characteristics of Rhodamine B using Co_3O_4 nanoparticles were studied using Rhodamine B. Following 90 min of irradiation, they are effectively reduced to 90% with Co_3O_4 nanoparticles under sunlight.

Keywords- Porous Co_3O_4 nanoparticles, Photocatalysis, Solution combustion approach.

1. INTRODUCTION

In the present scenario the ecological condition is getting worse day-by-day, and the shortage of clean water sources is alarming. The intense use of dyes in textile and leather industries is one of the reason for water pollution [1]. Discharge of toxins and pollutants into the natural water cycle would make the situation worse. Consequently, developing viable wastewater treatment technologies is need of the hour [2]. In recent times, photocatalysis is considered as one of the popular methods for waste water treatment due to its ability and efficiency to remove organic contaminants, using a photocatalyst under natural sunlight [3,4]. Tuning the morphology of nanomaterials is also very important for basic study of catalytic properties of a metal oxide [5,6]. In the midst of various semiconductor metal oxides, Cobalt oxide is well known and frequently used as a photocatalyst due to high photosensitivity, low cost and non-toxicity [7,8]. Cobalt oxide (Co_3O_4) finds enormous applications in rechargeable battery [9], magnetic materials [10], heterogeneous catalysts [11], gas sensors [12], supercapacitors [13] and energy storage [14]. Several methods for the cobalt oxide preparation have been studied just as sol-gel method [14], combustion method [15], hydrothermal method [16], micro emulsion method [17], spray pyrolysis technique [18], vapour deposition technique [19], thermal decomposition method [20] and microwave irradiation [21]. Synthesizing the metal oxide nanomaterials with porous structure will leads to high surface area resulting in high photocatalytic efficiency [22,23]. In this study, we approached a facile, fast and economical method for synthesizing Co_3O_4 nanoparticles by solution combustion method with large porous structures and small band gap which helps for absorbing large spectrum of sunlight irradiation resulting enhanced photocatalytic efficiency [11,24,25]. Photocatalytic degradation of Rhodamine B dye is investigated under natural sunlight. The synthesized Co_3O_4 nanoparticles were characterized by PXRD, DLS, SEM, EDAX, Raman spectroscopy and UV – visible techniques.

2. EXPERIMENTAL

A. Precursors

The chemical reagents like cobalt(III) nitrate hexahydrate [$CoN_3O_9{\cdot}6H_2O$], glycine [$C_2H_5NO_2$], sodium hydroxide [NaOH], nitric acid [HNO_3] and rhodamine B [$C_{28}H_{31}ClN_2O_3$] were purchased from Sigma Aldrich. All chemical substances were of high analytical quality and used without further purification. For all experiments deionized water was used.

B. Synthesis of Co3O4 nanoparticles

Co_3O_4 nanoparticles were synthesized using a facial solution combustion approach. The precursor Cobalt nitrate hexahydrate and the fuel glycine were used in such a way that the fuel oxidizer valence ratio equals one. Typically, 3 mmol of $Co(NO_3)_3.6H_2O$, 40 ml deionized water and appropriate amount of glycine were added to a beaker and vigorously stirred at room temperature for 30 mins. This mixture is then heated on a hot plate at 420°C and NaOH was added dropwise. After evaporation, the solution starts to boil foam and then ignite. The obtained dark brown powder was calcinated for 2 hours in muffle furnace at 600°C and stored for further characterization.

C. Analytical studies

The synthesized nanostructures were studied with powder X-ray diffraction (PXRD) (Rigaku smart Lab–II, CuKα radiation (λ=1.540598 Å)) to analyze the crystallinity of the product and its phase purity with a step size of 0.02° and 2θ range of 10 to 60°. The prepared sample morphology was examined by scanning electron microscope (SEM) (Hitachi (S-3400N)). The elemental analysis was undertaken by EDAX attached in the SEM. WITec alpha 300RA Raman Confocal Microscope was used to analyze the Raman spectra of the synthesized products in the wave number range of 100 to 1000 cm^{-1}. Shimadzu UV-2450 spectrophotometer was used to obtain the UV-vis spectra.

D. Photocatalytic activity assessment

The photocatalytic mineralization of Rhodamine B in presence of as-synthesized pure Co_3O_4 particles was tested under natural sunlight. 5 mg of photocatalyst was diffused in 100ml of RhB liquid solution (10 mg L^{-1}) of pH = 3. Ahead of irradiation, the mixture is sonicated for 10 mins in a sonicator through mixing with the dye and the solution is completely stirred in darkness to reach adsorption-desorption equilibrium. Under constant stirring, the reaction mixture is later exposed to direct sunlight. After various time intervals, the reaction mixture is analyzed and monitored by the Shimadzu UV-Vis spectrophotometer for degradation efficiency.

3. Results and Discussion

E. Structural Studies

The crystallinity and phase purity of porous Co_3O_4 nanoparticles were investigated by PXRD and related diffraction pattern is shown in fig 1. The diffraction peaks observed at (111), (220), (311), (222), (400), (422) and (511) in the 2θ range between 10 to 60° matches well with the standard Co_3O_4 values (JCPDS no. 65-3103). The data reports that Co_3O_4 crystallized as face-centered cubic (Fd3m) structure. No other peaks were found corresponding to other crystalline impurities. The size of the crystal was determined using Debye-Scherrer formula [26]:

$$D = 0.91\,\lambda / \beta \cos\theta \qquad (1)$$

Where 'λ' stands for wavelength (λ =0.154059 nm for CuKα), 'β' implies full width at half maximum intensity and 'θ' represents Bragg's angle.

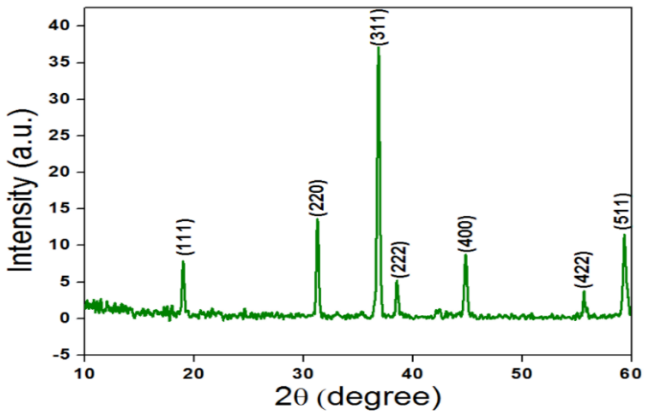

Figure 1. Powder XRD pattern of porous Co_3O_4 nanoparticles.

The particle size of Co_3O_4 nanoparticles estimated using dynamic light scattering technique with 0.01g of sample dispersed in 20 ml of water for 30 minutes. The corresponding particle size distribution curve had a mean particle diameter of 29 nm as shown in the fig 2. The particle size calculated by the analyzer is almost equal the average size estimated using XRD.

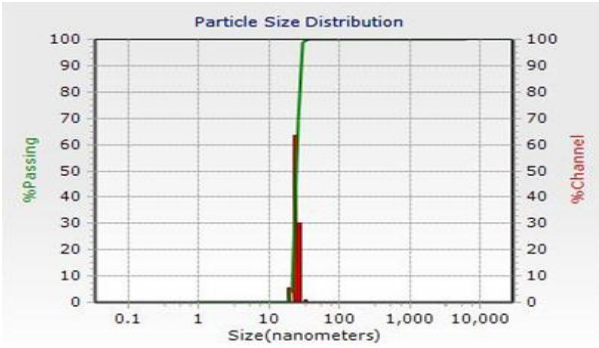

Figure 2. The particle size distributions curve of Co_3O_4 nanoparticles.

The morphological analysis of the product is carried out using scanning electron microscope. Fig 3 displays SEM images of pristine Co3O4 nanoparticles. Prepared Co_3O_4 exhibit micro-sized porous like morphology. This porosity of the sample might be due to the oxygen vacancies created by rapid ignition during synthesis, which shows higher surface area [27,28]. The porous network is attributed to solution combustion method during which gases were released [29]. This porous structure helps to increase the contact with pollutant nanoparticles and accordingly increases the efficiency of photocatalyst.

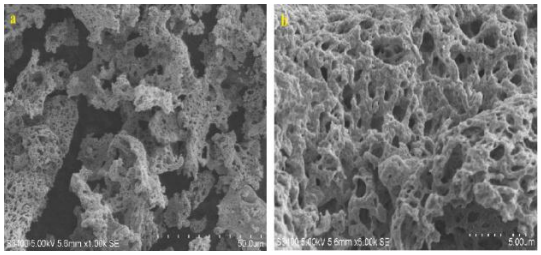

Figure 3. The SEM images of porous Co_3O_4nanoparticles at (a) 50µm and (b) 5µm magnification.

EDAX analysis confirms the purity and composition of the sample. The EDAX spectrum of Co_3O_4 shows Fig 4. The Co and O atoms are confirmed with atomic percentages of 45 and 55% respectively.

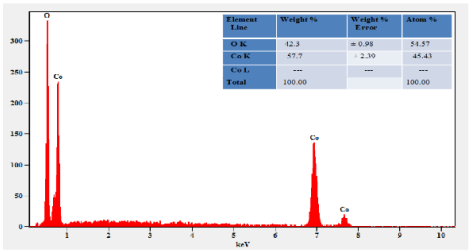

Figure 4. The EDAX spectrum of porous Co_3O_4 nanoparticles.

F. Optical studies

The microstructures of the Co_3O_4 nanoparticles were analyzed using Raman spectroscopy. All Raman peaks of Co_3O_4 at 185, 465, 506, 601 and 670 cm^{-1} were observed, which corresponds to F_{2g}, E_g, F_{2g}, F_{2g} and A_{1g} modes of crystalline porous Co_3O_4 nanoparticles respectively which matches fine with literature data [30].

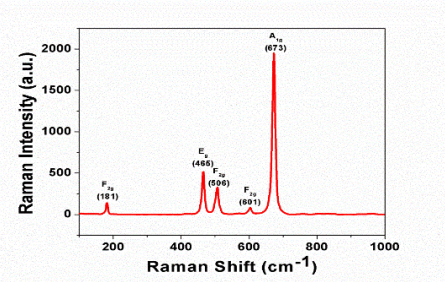

Figure 5. The Raman spectra of porous Co3O4 nanoparticles

The UV–visible spectra of Co_3O_4 were calculated to determine absorption properties. As shown in fig 6, the spectrum of porous Co_3O_4 has a broad visible light photoabsorption range between 350 and 800 nm. Moreover, the band gap of Co_3O_4 was determined using Tauc plot spectra derived from the UV – vis spectra [31]. The direct band gap of the porous Co3O4 sample was found to be 1.58 and 2.05 eV by extrapolating the linear area inside the Tauc plot [32].

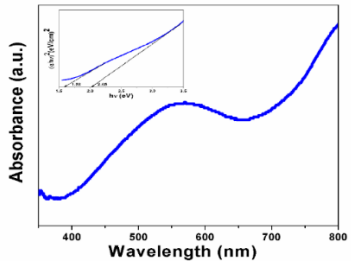

Figure 6. The absorbance spectrum and inset the direct band gap energy of porous Co_3O_4 nanoparticles.

G. Photocatalytic studies

The photocatalytic activity of the as-synthesized Co_3O_4 nanoparticles was measured for Rhodamine B dye (10 mg L^{-1}) by tracking its degradation under direct sunlight. Fig 7 displays the UV–visible absorption spectra of RhB under sunlight for different time interval. Fig 8(a) shows the RhB photodegradation curves as a result of the irradiation period over commercial Degussa TiO_2-P25 and textile dye photolysis. It is observed that the RhB degradation rate without any catalyst was observed to be 13% after 90 mins exposure to sunlight. The RhB degradation with the commercial TiO_2 – P25 catalyst had an efficiency of 70%, while the as-synthesized porous Co_3O_4 catalyst had degradation efficiency of 90% in 90 mins irradiated under direct sunlight. The porous structure of Co_3O_4 nanoparticles plays a significant role in improving photocatalytic activity [31]. Furthermore, Fig 8(b) gives a quantitative understanding about the kinetics of the degradation reaction which uses the pseudo-first-order model [33] given by:

$$\ln(C_o \backslash C) = kt \qquad (1)$$

Where, C and C_o represents the dye concentrations in suspension at time t and 0 respectively. 'k' stands for the rate constant for time 't' of pseudo-first-order.

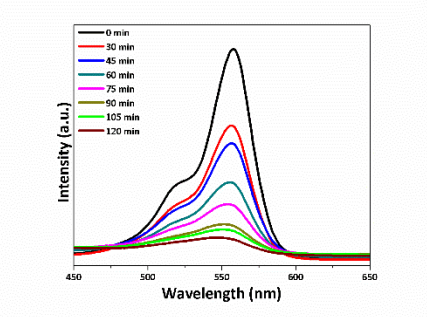

Figure 7. Absorption spectrum of RhB in Co_3O_4 nanoparticles at different time interval.

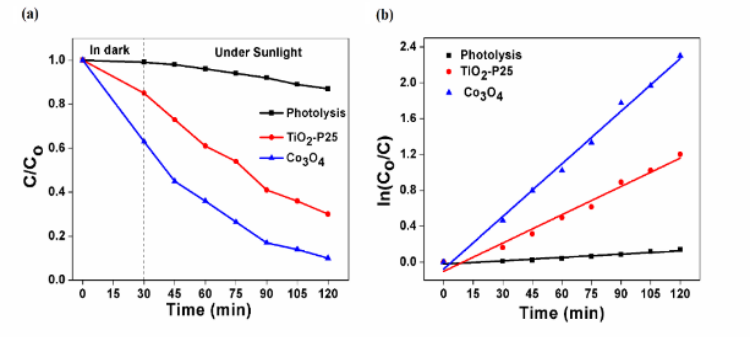

Figure 8. (a) RhB dye adsorption and photocatalytic degradation under sunlight. (b) The degradation kinetics of RhB under sunlight

4. PHOTOCATALYTIC MECHANISM

Fig 9 shows the schematic mechanism of the porous Co_3O_4 nanoparticles photocatalytic degradation of the RhB dye under sunlight irradiation. Porous $Co_3O_4$with energy gap of 2.05 eV will absorb the photon energy from sunlight causing the photoelectrons in the valence band excite to the conduction band forming positively charged holes and electrons (Eq. (1)). The photogenerated holes on the valence band VB of porous Co_3O_4 will react with water molecule to form hydroxyl radical (Eq. (2)). The generated active •OH radicals effectively react with RhB to produce CO_2, H_2O or other products (Eq. (3)).

$$Co_3O_4 + h\nu \rightarrow Co_3O_4 + (e^-_{CB} + h^+_{VB}) \quad (1)$$

$$h^+_{VB} + H_2O \rightarrow {}^{\bullet}OH \quad (2)$$

$${}^{\bullet}OH + RhB \rightarrow \text{Inorganic products } (CO_2, H_2O, \ldots) \quad (3)$$

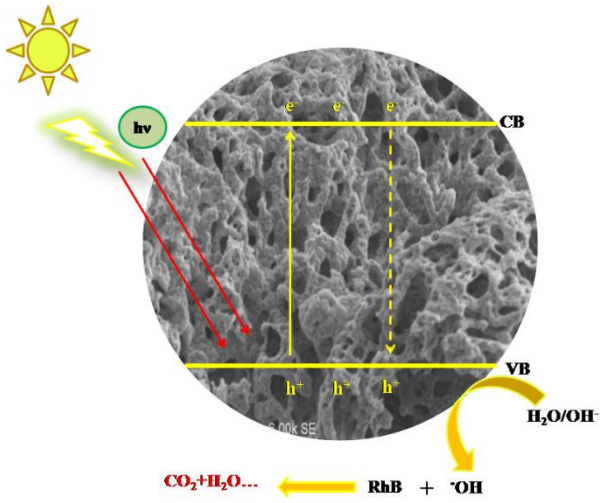

Figure 9. The schematic mechanism of the porous Co_3O_4 nanoparticles photocatalytic degradation of RhB dye.

5. CONCLUSION

In this work, porous Co_3O_4 nanoparticles were successfully synthesized using solution combustion method. PXRD, EDAX and Raman analyses confirm the Co_3O_4 nanostructure. The DLS analyses confirmed the size 29 nm of the prepared sample. The SEM photographs display the porous structure of Co_3O_4 nanoparticles showing higher surface area due to oxygen vacancies. UV–visible analysis shows the broad visible-light absorption range between 350 and 800 nm for the porous structure and showing the band gaps energy of 1.58 and 2.05 eV. The expansion of the absorption in the visible region shows enhanced photodegradation [34] of the RhB dye using porous Co_3O_4 photocatalyst than commercial Degussa

TiO_2 – P25. Thus, Co_3O_4 nanoparticles are a potential sunlight active photocatalyst for the degradation of RhB dye present in the industrial wastes.

6. ACKNOWLEDGMENT

The authors are thankful to the National Single Crystal Diffractometer Facility, DoS in Physics, CPEPA and DST-Purse, Vijnana Bhavana, University of Mysore, Mysuru.

7. REFERENCES

[1] Kant, R.: Textile dyeing industry an environmental hazard. Natural Sciences **04**, 22–26 (2012).
[2] Muga, H. E., Mihelcic, J. R.: Sustainability of wastewater treatment technologies. Journal of Environmental Management **88**, 437–447 (2008).
[3] Herrmann, J. M., Guillard, C., Pichat, P.: Heterogeneous photocatalysis : an emerging technology for water treatment. Catalysis Today **17**, 7–20 (1993).
[4] Nan Chong, M., Jin, B., Chow, C. W., Saint, C.: Recent developments in photocatalytic water treatment technology: A review. Water Research **44**, 2997–3027 (2010).
[5] Yang, X. et al.: Tuning the Morphology of g-C_3N_4 for Improvement of Z-Scheme Photocatalytic Water Oxidation. ACS Applied Material and Interfaces **7**, 15285–15293 (2015).
[6] Pascariu, P., Tudose, I. V., Suchea, M.: Surface Morphology Effects on Photocatalytic Activity of Metal Oxides Nanostructured Materials Immobilized onto Substrates. Journal of Nanoscience and Nanotechnology **19**, 295–306 (2018).
[7] Rosen, J., Hutchings, G. S., Jiao, F.: Ordered Mesoporous Cobalt Oxide as Highly Efficient Oxygen Evolution Catalyst. Journal of the American Chemical Society **135**, 4516–4521 (2013).
[8] Lou, X., Han, J., Chu, W., Wang, X., Cheng, Q.: Synthesis and photocatalytic property of Co_3O_4 nanorods. Materials Science and Engineering: B **137**, 268–271 (2007).
[9] Yao, X. et al.: Co_3O_4 nanowires as high capacity anode materials for lithium ion batteries. Journal of Alloys and Compounds **521**, 95–100 (2012).
[10] Mate, V. R., Shirai, M., Rode, C. V.: Heterogeneous Co_3O_4 catalyst for selective oxidation of aqueous veratryl alcohol using molecular oxygen. Catalysis Communication **33**, 66–69 (2013).
[11] Cui, Y., Wen, Z., Sun, S., Lu, Y., Jin, J.: Mesoporous Co_3O_4 with different porosities as catalysts for the lithium-oxygen cell. Solid State Ionics **225,** 598–603 (2012).
[12] Park, J., Shen, X., Wang, G.: Solvothermal synthesis and gas-sensing performance of Co_3O_4 hollow nanospheres. Sensors and Actuators B: Chemical **136**, 494–498 (2009).
[13] Meher, S. K., Rao, G. R.: Ultralayered Co_3O_4 for High-Performance Supercapacitor Applications. The Journal of Physical Chemistry C **115**, 15646–15654 (2011).
[14] Švegl, F., Orel, B., Hutchins, M. G., Kalcher, K.: Structural and spectroelectrochemical investigations of sol-gel derived electrochromic spinel Co_3O_4 films. Journal of the Electrochemical Society **143**, 1532–1539 (1996).
[15] Venkateswara Rao, K., Sunandana, C. S.: Co_3O_4 nanoparticles by chemical combustion: Effect of fuel to oxidizer ratio on structure, microstructure and EPR. Solid State Communication **148**, 32–37 (2008).
[16] Li, L. et al.: A facile hydrothermal route to synthesize novel Co_3O_4 nanoplates. Materials Letters **62**, 1507–1510 (2008).
[17] Morsy, S. M. I., Shaban, S. A., Ibrahim, A. M., Selim, M. M.: Characterization of cobalt oxide nanocatalysts prepared by microemulsion with different surfactants, reduction by hydrazine and mechanochemical method. Journal of Alloys and Compounds **486**, 83–87 (2009).
[18] Kim, D. Y., Ju, S. H., Koo, H. Y., Hong, S. K., Kang, Y. C.: Synthesis of nanosized Co_3O_4 particles by spray pyrolysis. Journal of Alloys and Compounds **417**, 254–258 (2006).
[19] Rumplecker, A., Kleitz, F., Salabas, E.-L., Schüth, F.: Hard Templating Pathways for the Synthesis of Nanostructured Porous Co_3O_4. Chemistry of Materials **19**, 485–496 (2007).
[20] Mohandes, F., Davar, F., Salavati-Niasari, M.: Preparation of Co_3O_4 nanoparticles by nonhydrolytic thermolysis of [Co(Pht)(H_2O)]n polymers. Journal of Magnetism and Magnetic Materials **322**, 872–877 (2010).
[21] Bhatt, A. S., Bhat, D. K., Tai, C. W., Santosh, M. S.: Microwave-assisted synthesis and magnetic studies of cobalt oxide nanoparticles. Materials Chemistry and Physics **125**, 347–350 (2011).
[22] Chandrappa, G. T., Steunou, N., Livage, J.: Materials chemistry: Macroporous crystalline vanadium oxide foam. Nature **416**, 702 (2002).
[23] Hezam, A. *et al.*: Sunlight-Driven Combustion Synthesis of Defective Metal Oxide Nanostructures with Enhanced

Photocatalytic Activity. ACS Omega **24**, 20595-20605 (2019).
[24] Wang, J. et al.: Oxygen Vacancy Induced Band-Gap Narrowing and Enhanced Visible Light Photocatalytic Activity of ZnO. ACS Applied Materials & Interfaces **4**, 4024–4030 (2012).
[25] Zhou, H., Qu, Y., Zeid, T., Duan, X.: Towards highly efficient photocatalysts using semiconductor nanoarchitectures. Energy and Environmental Science **5,** 6732–6743 (2012).
[26] Hall, B. D., Zanchet, D., Ugarte, D.: Estimating nanoparticle size from diffraction measurements. Journal of Applied Crystallography **33**, 1335–1341 (2000).
[27] Xu, L. et al.: Plasma-Engraved Co_3O_4 Nanosheets with Oxygen Vacancies and High Surface Area for the Oxygen Evolution Reaction. Angewandte Chemie - International Edition **55**, 5277–5281 (2016).
[28] Liotta, L. F. *et al.*: Total oxidation of propene at low temperature over Co_3O_4-CeO_2 mixed oxides: Role of surface oxygen vacancies and bulk oxygen mobility in the catalytic activity. Applied Catalysis A: General **347**, 81–88 (2008).
[29] Mukasyan, A. S., Epstein, P., Dinka, P.: Solution combustion synthesis of nanomaterials. Proceedings of the Combustion Institute **31 II**, 1789–1795 (2007).
[30] Diallo, A., Beye, A. C., Doyle, T. B., Park, E., Maaza, M.: Green synthesis of Co_3O_4 nanoparticles via Aspalathus linearis: Physical properties. Green Chemistry Letters and Reviews **8**, 30–36 (2015).
[31] Feng, Y., Lin, S., Huang, S., Shrestha, S., Conibeer, G.: Can Tauc plot extrapolation be used for direct-band-gap semiconductor nanocrystals?. Journal of Applied Physics **117**, (2015).
[32] Gu, F., Li, C., Hu, Y., Zhang, L.: Synthesis and optical characterization of Co_3O_4 nanocrystals. Journal of Crystal Growth **304**, 369–373 (2007).
[33] Kumar, K. V., Porkodi, K., Rocha, F.: Langmuir-Hinshelwood kinetics - A theoretical study. Catalysis Communication **9**, 82–84 (2008).
[34] Sadiq, M. M. J., Nesaraj, A. S.: Reflux condensation synthesis and characterization of Co_3O_4 nanoparticles for photocatalytic applicaions. Iranian Journal of Catalysis **4**, 219–226 (2014).